

Injectable chitosan-platelet-rich plasma implants to promote tissue regeneration: *in vitro* properties, *in vivo* residence, degradation, cell recruitment and vascularization

A. Chevrier¹, V. Darras¹, G. Picard¹, M. Nelea¹, D. Veilleux², M. Lavertu¹, C.D. Hoemann^{1,2} and M.D. Buschman^{1,2*}

¹Chemical Engineering Department, Polytechnique Montreal, Montreal, QC, Canada

²Biomedical Engineering Institute, Polytechnique Montreal, Montreal, QC, Canada

Abstract

The purpose of this study was to develop freeze-dried chitosan formulations that can be solubilized in platelet-rich plasma (PRP) to form injectable implants for tissue repair. A systematic approach to adjust formulation parameters, including chitosan number average molar mass (M_n), chitosan concentration and lyoprotectant concentration, was undertaken to identify compositions that would rapidly (< 1 min) and completely solubilize in PRP, would have paste-like handling properties upon solubilization and coagulate rapidly (< 5 min) to form solid chitosan-PRP hybrid implants that are stable and homogenous. Freeze-dried cakes containing calcium chloride, as well as distinct chitosan M_n , chitosan concentration and lyoprotectant concentration, were prepared. PRP was used to solubilize the freeze-dried cakes and assess *in vitro* and *in vivo* performance, the latter as dorsal subcutaneous injections into New Zealand White rabbits. Freeze-dried polymer formulations containing low and medium chitosan M_n and concentrations were rapidly and completely solubilized in PRP. The paste-like chitosan-PRP mixtures coagulated quickly to form solid chitosan-PRP hybrids, which retracted much less than PRP-only controls. Homogeneous dispersion of chitosan within the hybrid clots was strongly dependent on chitosan M_n , and occurred only with medium M_n chitosan. Chitosan-PRP hybrid clots were resident subcutaneously *in vivo* until at least 2 weeks while PRP controls were quickly degraded in one day. Compared to PRP alone, chitosan-PRP hybrids had much greater capacity to induce local cell recruitment accompanied by angiogenesis, suggesting a strong potential for their use in regenerative medicine. Copyright © 2017 John Wiley & Sons, Ltd.

Received 30 June 2016; Revised 24 November 2016; Accepted 9 January 2017

Keywords chitosan; platelet-rich plasma; injectable implants; tissue repair; biocompatibility

1. Introduction

Chitosan is a linear polysaccharide composed of glucosamine and N-acetyl-glucosamine units that has been used for several biomedical and pharmaceutical applications. Chitosan is typically soluble only in acidic conditions, thus limiting its use in physiological applications. A previously discovered approach to partially circumvent this limitation was to use a glycerol phosphate (GP) buffer which can solubilize chitosan solution in acidic conditions at a pH close to 7 without precipitating the polymer (Chenite *et al.*, 2000). Chitosan-GP was then mixed with whole blood to form blood/polymer solutions that coagulate (Marchand *et al.*, 2009) to form hybrid polymer/blood clots that significantly resist platelet-mediated clot retraction (Hoemann *et al.*, 2007). Chitosan-GP/blood implants

were injected in a liquid format over surgically prepared cartilage defects where they solidified *in situ* and improved repair compared to bone marrow stimulation (microfracture) (Hoemann *et al.*, 2005; Hoemann *et al.*, 2007). Some of the mechanisms responsible for improved repair *in vivo* include increased recruitment of cells from the subchondral bone (Chevrier *et al.*, 2007), increased transient vascularization and bone remodeling (Chevrier *et al.*, 2007; Hoemann *et al.*, 2007; Hoemann *et al.*, 2010), promotion of a beneficial phenotype of alternatively activated macrophages (Hoemann *et al.*, 2010) and increased osteoclast activity, leading to better repair tissue integration (Chen *et al.*, 2011). The use of chitosan-GP/blood implants (BST-CarGel® a medical device from Smith and Nephew, MA, USA) in conjunction with microfracture was also found to be superior to microfracture alone in a randomized controlled clinical trial (Stanish *et al.*, 2013; Shive *et al.*, 2015), leading to the approval and distribution of this formulation for cartilage repair in several countries.

Long-term stability and ease of sterilization are some of the limitations of the current chitosan-GP solution-based

*Correspondence to: Michael D. Buschmann, Department of Chemical Engineering, Polytechnique Montreal, PO Box 6079 Succ Centre-Ville, Montreal, Quebec, Canada, H3C 3A7. E-mail: michael.buschmann@polymtl.ca

system. Long-term storage of chitosan mixed with GP is precluded by the gradual transition of the system from liquid to gel form (Lavertu *et al.*, 2008). Storage of the chitosan and GP components separately is also problematic due to acid hydrolysis of chitosan (Varum *et al.*, 2001). Although the rate of chitosan hydrolysis and degradation may be slowed by storing the chitosan solutions at cold temperatures (Nguyen *et al.*, 2008), decreases in viscosity are unavoidable. Finally, the high viscosity of the chitosan solution in the chitosan-GP system prevents sterilization by filtration, thus requiring steam sterilization leading to variable decreases in viscosity (Jarry *et al.*, 2001). In principle, the above limitations could be overcome by freeze-drying (lyophilization) of the polymer to produce a freeze-dried cake.

Platelet-rich plasma (PRP) has been used to deliver platelet-derived growth factors for different applications (Lu *et al.*, 2008). PRP injections are currently being used by orthopaedic surgeons for the treatment of osteoarthritis (Kon *et al.*, 2013), meniscus tears (Griffin *et al.*, 2015) and rotator cuff tears (Chahal *et al.*, 2012), but results have been inconsistent so far. Liquid suspensions of anticoagulated platelet concentrates can be activated to coagulate by using thrombin, calcium chloride (CaCl_2) or other activators to form solid implants. Some of the current shortcomings of PRP include variability in biological activity due to variability in donor parameters and in concentration techniques (Zumstein *et al.*, 2011; Ahmad *et al.*, 2012). It has been known for years that PRP is physically unstable once coagulated, displaying both a very high clot retraction to a fraction of its original volume (Chao *et al.*, 1976) and being susceptible to rapid lysis in many physiological environments including the synovial joints. Previous data, using whole blood rather than PRP, found that a structurally more stable clot could be generated by incorporating chitosan (Hoemann *et al.*, 2007). In addition to producing a more stable PRP implant, direct incorporation of freeze-dried chitosan into PRP could overcome the short shelf-life of prior liquid chitosan formulations. Furthermore, the implementation of PRP rather than whole blood is expected to increase the bioactivity of the implants, due to the concentration of platelet-derived growth factors, and to improve repair outcomes in cartilage, meniscus and rotator cuff repair.

The purpose of this study was to identify freeze-dried chitosan formulations that can be solubilized in PRP to form injectable gelling implants for tissue repair. Such a regenerative medicine system could overcome the previous shortcomings of solution-based chitosan systems, as well as improve the regenerative capacity of PRP by physically stabilizing PRP *in vivo* through reinforcement with a degradable and biocompatible polymer. A systematic approach to adjust formulation parameters, including chitosan number average molar mass (M_n), chitosan concentration and lyoprotectant concentration, was undertaken to identify compositions that met pre-defined performance criteria. We aimed to

identify formulations that would rapidly and completely solubilize in PRP, would have paste-like handling properties upon solubilization and would coagulate rapidly to form solid chitosan-PRP hybrid implants that are stable and homogenous. Our starting hypotheses were the following. First, chitosan M_n , chitosan concentration and lyoprotectant concentration would control performance of solubilized mixtures. Second, and more specifically, increasing chitosan M_n and chitosan concentration in the freeze-dried cakes would improve the paste-like properties of the chitosan-PRP mixtures, but would hinder cake solubility. Finally, increasing lyoprotectant concentration in the freeze-dried cakes would improve cake properties but lead to high osmolality upon solubilization, which could induce deleterious effects including cell necrosis upon *in vivo* implantation.

2. Materials and methods

2.1. Preparation of freeze-dried chitosan formulations

Chitosan (raw material purchased from Marinard) was deacetylated with sodium hydroxide and then depolymerized with nitrous oxide to obtain different chitosans, which were then characterized by NMR spectroscopy and size-exclusion chromatography/multi-angle laser light scattering for degree of deacetylation and molar mass, respectively (Lavertu *et al.*, 2003; Nguyen *et al.*, 2009). All chitosans had degrees of deacetylation between 80% and 85% and were categorized as having low M_n (between 4 and 11 kDa), medium M_n (between 28 and 56 kDa) or high M_n (between 79 and 154 kDa, measured after autoclave sterilization). Chitosans were dissolved in HCl overnight at room temperature (HCl concentration adjusted to obtain 60% protonation of the amino groups) to obtain solutions containing low, medium or high concentrations of chitosan, 0.56% (w/v), 1% (w/v) or 1.5% (w/v), respectively. Since chitosans of high M_n cannot be filtered, they were sterilized by autoclaving for 10 min, which decreased M_n by an average 30% to reach the values reported above. Chitosans of low or medium M_n were sterilized by filtration, which we have shown causes no decrease in M_n . Trehalose (Sigma, Product N° T-0167) or mannitol (Sigma, Product N° M-1902) were added to the chitosan solutions as lyoprotectants (widely used in the pharmaceutical industry to protect the material during freeze-drying) to obtain final concentrations ranging from 1% (w/v) to 10% (w/v). Calcium chloride (Sigma, Product N° C-5670) was also added to obtain a final concentration of 42.2 mM as in previously published methods (Anitua *et al.*, 2008). Rhodamine-chitosan tracers (Ma *et al.*, 2008) of corresponding M_n were filter-sterilized and added to the formulations for imaging purposes before dispensing in individual glass vials for freeze-drying. pH of the different chitosan formulations was 6.16 ± 0.44 (mean \pm SD) prior to freeze-drying. The freeze-drying cycle consisted of: 1) ramped freezing

to -40°C in 1 h, then isothermal for 2 h at -40°C ; 2) -40°C for 48 h at 100 millitorrs; and 3) ramped heating to 30°C in 12 h, then isothermal for 6 h at 30°C , at 100 millitorrs.

2.2. Isolation of platelet-poor-plasma (PPP) and platelet-rich plasma (PRP)

All subjects enrolled in this research responded positively to an Informed Consent Form which was approved by the Polytechnique Montreal institutional committee (Comité d'éthique à la recherche avec des êtres humains) (#CÉR-10/11-08; initial date of approval, 16 February 2011). Sodium citrate anti-coagulated whole blood (final citrate concentration in blood, 12.9 mM) was collected from five human donors (with some donors sampled more than once) and centrifuged at 160 g for 10 min and then at 400 g for 10 min to extract leukocyte-platelet-rich plasma (L-PRP, which contains leukocytes and a fraction of erythrocytes) and also platelet-poor plasma (PPP). This isolation method typically yields a PRP with $\sim 0.2x$ the amount of erythrocytes, $\sim 0.8x$ the amount the leukocytes and $\sim 3x$ more platelets as compared to whole blood. pH and osmolality of PRP and PPP were measured and no significant difference was found between the two (Tables 2A and 2B).

2.3. Assessment of cake solubility, osmolality and pH measurements

Freeze-dried chitosan cakes (1 ml chitosan formulation) were solubilized and shaken vigorously for 10 seconds with 1 ml PPP, since the erythrocyte fraction present in PRP prevents visual assessment of solubility. Osmolality and pH of the chitosan-PPP mixtures were immediately measured. Chitosan-PRP mixtures are expected to have post-solubilization properties similar to those of chitosan-PPP, since osmolality and pH of PPP and PRP are the same (Tables 2A and 2B).

2.4. Assessment of paste-like properties of chitosan-PRP formulations through a runniness test

Freeze-dried chitosan cakes (1 ml chitosan formulation) were solubilized with 1 ml PRP, and runniness was assessed by placing a 30 μl drop of each formulation immediately after solubilization onto a rigid piece of plastic fixed at 38 degrees to horizontal. Controls were PRP recalcified with 42.2 mM of calcium chloride. Photos were taken at fixed times and the distance the drop travelled down the piece of plastic was measured using Image J 1.47v.

2.5. Assessment of clotting properties of chitosan-PRP formulations through thromboelastography

Freeze-dried chitosan cakes were solubilized with PRP and 360 μl of each formulation was immediately loaded

into a thromboelastograph cup, and TEG tracings were recorded for 1 h using a TEG Model 5000 (Haemoscope Corp). The clot reaction time (R) is the time in minutes from the start of the tracing to the point where the branches have diverged 2 mm. The maximal amplitude (MA) is the maximal distance in mm between the two diverging branches and corresponds to clot strength. Controls were PRP recalcified with 42.2 mM of calcium chloride.

2.6. Assessment of hybrid clot stability

Formulations solubilized in PRP were dispensed into glass tubes and placed in a heat block set at 37°C . After 60 min, the serum expressed from the clots was removed and % mass lost was quantified by gravimetric measurements. Controls were PRP recalcified with 42.2 mM of calcium chloride. Hybrid chitosan-PRP clots and control PRP clots were then fixed in 10% neutral buffered formalin (NBF) for further histological assessment.

2.7. Assessment of hybrid clot homogeneity through histology

Rhodamine-chitosan tracers were added to the freeze-dried cakes to allow detection of chitosan within the hybrid clots with epifluorescence microscopy. Thick razor blade sections (~ 1 mm) were observed with a Zeiss Axiovert inverted microscope and low magnification pictures encompassing the whole clot were taken with a Princeton Instruments camera, Model RTE/CCD-1317-k/2, to evaluate chitosan distribution in the hybrid clots. Brightfield pictures were also acquired using a Zeiss Stemi microscope equipped with a Sony 3CCD colour video camera, Model DXC-390P.

2.8. Assessment of *in vivo* responses

Canadian Council on Animal Care guidelines for the care and use of laboratory animals were observed. The study was approved by the University of Montreal committee (Comité de déontologie de l'expérimentation sur les animaux) (#13-129; initial date of approval, 27 August 2013). Solubilized formulations were injected subcutaneously into the backs of New Zealand White rabbits ($n = 11$ rabbits in total, four female retired breeders and seven males, 3–4 months old) to assess implant biodegradability and biocompatibility (Table 1). Freeze-dried chitosan cakes (300 μl chitosan formulation) were solubilized with 300 μl autologous PRP for dorsal subcutaneous injections using 26 gauge needles (each injection consisted of 150 μl chitosan-PRP formulation). A total of eight different chitosan-PRP formulations were injected (Table 1). The first four animals received eight injections each and were sacrificed at day 1 ($n = 2$) and day 3 ($n = 2$). One animal received 12 injections and was sacrificed at day 14. The remaining animals received 16 injections each and were sacrificed at day 1 ($n = 2$),

Table 1. Study design for subcutaneous implantation. Freeze-dried chitosan formulations containing chitosan, trehalose as lyoprotectant, and calcium chloride as clot activator were reconstituted in autologous PRP for dorsal subcutaneous injections into 11 New Zealand White rabbits. Controls were PRP recalcified with calcium chloride and liquid chitosan-GP/blood implants. Implants were histologically assessed at 1, 3, 7 and 14 days post surgery

| Subcutaneous injection study ($n = 11$ rabbits) with freeze-dried chitosan-PRP implants Animals were sacrificed at day 1 ($n = 4$), day 3 ($n = 2$), day 7 ($n = 2$) and day 14 ($n = 3$) | | | | | | | |
|---|----------------|--------------|----------|---------------------|------------------------|------------------|--------------------------------------|
| CS DDA (%) | CS M_n (kDa) | CS % (w/vol) | HCl (mM) | Trehalose % (w/vol) | CaCl ₂ (mM) | β -GP (mM) | Number of injections |
| 80.6 | 36-50 | 0.56 | 16 | 1 | 42.2 | 0 | 12 injections in 3 different rabbits |
| 80.6 | 36-50 | 0.56 | 16 | 2 | 42.2 | 0 | 16 injections in 5 different rabbits |
| 80.6 | 36-50 | 0.56 | 16 | 4 | 42.2 | 0 | 16 injections in 5 different rabbits |
| 80.6 | 36-50 | 0.56 | 16 | 6 | 42.2 | 0 | 8 injections in 3 different rabbits |
| 80.6 | 36-50 | 1 | 29 | 1 | 42.2 | 0 | 12 injections in 3 different rabbits |
| 80.6 | 36-50 | 1 | 29 | 2 | 42.2 | 0 | 16 injections in 5 different rabbits |
| 80.6 | 36-50 | 1 | 29 | 4 | 42.2 | 0 | 16 injections in 5 different rabbits |
| 80.6 | 36-50 | 1 | 29 | 6 | 42.2 | 0 | 8 injections in 3 different rabbits |
| 80.6 | ~150 | 0.42 | 16 | 0 | 0 | 25 | 14 injections in 7 different rabbits |

day 7 ($n = 2$) and day 14 ($n = 2$). The injection sites were varied on each animal to avoid site-dependant outcomes. Controls were autologous PRP recalcified with 42.2 mM calcium chloride. In addition, implants consisting of 150 μ l of chitosan-GP/blood were also injected. These were prepared by mixing 1.5 ml of a solution containing 1.62% w/v Chitosan (80% DDA, ~150 kDa), 100 mM glycerol phosphate (Sigma, Product N° G-9891) and 65 mM HCl with 4.5 ml of whole blood immediately prior to implantation. Implants were assessed histologically at days 1, 3, 7 and 14 post injection ($n = 2$ –8 implants of each formulation at each time point). Animals received a ketamine/xylazine injection for anesthesia prior to injection but no analgesic was given post operatively. The rabbits did not experience any significant weight loss throughout the study period.

2.9. Histoprocessing, staining and immunostaining of subcutaneous implants

Implants were fixed in 10% NBF, paraffin-embedded and sectioned at 5 μ m using a Leica RM2155 microtome. Paraffin sections were stained with Weigert iron hematoxylin and 0.04% (w/v) Fast Green or with Hoeschst 33258. For immunohistochemistry, sections were dewaxed and antigen retrieval was performed by heating at 60°C in 10 mM Tris pH 10, followed by blocking for 1 h at room temperature in 20% goat serum/PBS/0.1% Triton X-100. Primary antibodies (Anti-Rabbit Macrophage Clone RAM11, Dako, catalogue No M0633 and Anti-Human CD31 Clone JC70A, Dako, Catalogue No M0823) were diluted 1:50 and 1:20, respectively, in 10% goat serum/PBS/0.1% Triton X-100 and incubated overnight at 4°C. Secondary antibody (Biotinylated Goat Anti-Mouse IgG, Sigma, Catalogue No B-7151) was diluted 1:200 in 10% goat serum/PBS/0.1% Triton X-100 and incubated for 1 h at room temperature. Revelation was with the ABC-AP and AP Red substrate kits (Vector Laboratories) and counterstaining was done with Weigert iron hematoxylin. Stained and immunostained slides were scanned at 40X with a Nanozoomer RS scanner (for brightfield) or a

Nanozoomer HT scanner (for fluorescence) (Hamamatsu, Japan). NDPView (Hamamatsu) was used to export images for further analysis.

2.10. Cell stereology

Eight 80X (achieved with digital zoom) magnification images were systematically acquired from each fast-green-stained (for nucleated cells counting) and immunostained (for Ram11-positive macrophages counting) section. Four images were acquired at the edge of the implants (left, top, right, bottom) and four images were acquired inside the implants. A 20 \times 12 grid containing 240 points with square sizes of 8.33 μ m \times 8.33 μ m was superimposed on each image with Image J 1.47v. Point counting was performed and Vv (Volume density) of nucleated cells and RAM11-positive macrophages was obtained by applying $Vv = \sum P \text{ cell type} / \sum P \text{ total}$ (Griffiths, 1993). The average of four acquired images was calculated to obtain Vv at the edge and in the middle of each implant.

2.11. Statistical analysis

Formulations were grouped according to chitosan M_n (labeled low, medium and high, as described above), chitosan concentration (0.56% w/v labeled low and 1% w/v labeled medium) and lyoprotectant concentration (1–2% w/v labeled low, 4% w/v labeled medium and 6% w/v labeled high). All statistical analyses were performed with SAS Enterprise Guide 5.1 and SAS 9.3. Data in the Tables are presented as mean \pm SD. Data in the Figures are presented as median (line); Box: 25th and 75th percentile; Whisker: Box to the most extreme point within 1.5 interquartile range. The Mixed model task in SAS Enterprise Guide was used to compare the different groups with post-hoc analysis to look at pairwise differences. Fixed effects were chitosan M_n , chitosan concentration and lyoprotectant concentration while donor was a random effect, as some donors were sampled more than once. Correlations between the different performance criteria assessed and chitosan M_n , chitosan

concentration and lyoprotectant concentration were analysed by calculating the Pearson correlation coefficients (r). p values <0.05 were considered significant.

3. Results

3.1. Freeze dried chitosan can be solubilized rapidly in PRP and coagulate

There was less cake shrinkage when lyoprotectant concentration was increased or when cakes contained mannitol (Figure 1a–c). Freeze-dried chitosan formulations containing low and medium chitosan M_n and concentrations were rapidly and completely solubilized in PPP (Figure 1g–i) and in PRP. Formulations containing 1.5% (w/v) chitosan were only partially soluble (Figure 1g, h) and were therefore excluded from further analysis. Coagulation successfully occurred post

solubilization in PRP when lyoprotectant concentration in the cakes was between 1% (w/v) and 6% (w/v) (Figure 1d shows a TEG curve for 2% w/v trehalose). A significant decrease in clot maximal amplitude was seen with formulations containing 8% (w/v) lyoprotectant (Figure 1e) and coagulation was inhibited when cakes had 10% (w/v) lyoprotectant (Figure 1f).

3.2. Osmolality can be controlled by lyoprotectant concentration

As expected, osmolality of solubilized chitosan formulations increased with the lyoprotectant concentration and osmolality was greater for formulations containing mannitol compared to trehalose, due to the lower molar mass of mannitol (Table 2A). Chitosan-PRP formulations had osmolalities ranging from 1.4x that of PRP to more than twice that of PRP (Table 2A). Chitosan

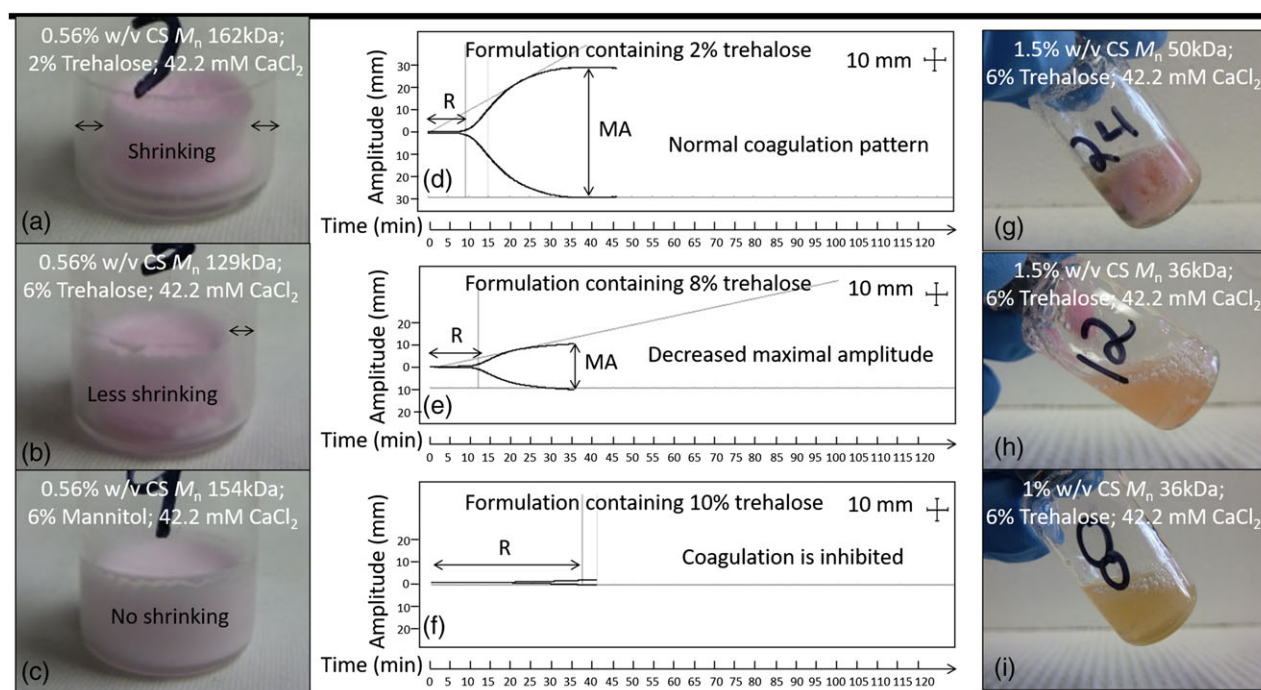


Figure 1. Optimization of freeze-dried chitosan formulations. Increasing lyoprotectant concentration or adding mannitol rather than trehalose to chitosan formulations produced freeze-dried cakes that shrank less and were space-filling (compare panel b to a and panel c to b). TEG tracings (cross, 10 mm) vs. time (in minutes) (panels d to f). Clot reaction time R is the time in minutes from initiation of the tracing to the point where branches have diverged 2 mm. Maximal amplitude (MA) is the maximal distance in mm between the two diverging branches and corresponds to clot strength. Increasing lyoprotectant concentration in freeze-dried chitosan formulations decreased chitosan-PRP hybrid clot strength, as assessed by thromboelastography (compare panels d and e), and inhibited coagulation at the highest concentration tested (panel f). Decreasing chitosan M_n and chitosan concentration improved the solubility of freeze dried cakes from insoluble (panel g), to partially soluble (panel h) and fully soluble (panel i). Freeze-dried cakes are pink because rhodamine-chitosan tracers of similar M_n were added to each formulation for imaging purposes. [Colour figure can be viewed at wileyonlinelibrary.com]

Table 2A. Osmolality of formulations post reconstitution with PPP. Data are presented as mean \pm SD. n was between 3 and 13 for each formulation. As expected, osmolality increased as lyoprotectant concentration increased, and osmolality was greater for formulations containing mannitol as compared to those containing trehalose

| Lyoprotectant concentration | Chitosan concentration 0.56% w/v | | Chitosan concentration 1% w/v | | Freshly isolated PPP | Freshly isolated PRP |
|-----------------------------|------------------------------------|--------------|---------------------------------|--------------|----------------------|----------------------|
| | Trehalose | Mannitol | Trehalose | Mannitol | | |
| 1% w/v | 424 \pm 8 | N/D | 450 \pm 8 | N/D | | |
| 2% w/v | 474 \pm 16 | 548 \pm 31 | 473 \pm 14 | 510 \pm 22 | 301 \pm 4 | 305 \pm 15 |
| 4% w/v | 501 \pm 51 | 590 \pm 53 | 522 \pm 12 | 639 \pm 37 | | |
| 6% w/v | 607 \pm 22 | 773 \pm 35 | 601 \pm 26 | 702 \pm 95 | | |

solutions had a pH between 6.02 and 6.35 before freeze-drying. As expected, pH increased after solubilization, ranging between 6.75 and 7.11 (Table 2B).

3.3. Chitosan-PRP mixtures are paste-like, clot in a few minutes and do not retract, unlike PRP alone

Chitosan-PRP formulations were more paste-like than recalcified PRP (Figure 2), and increasing chitosan M_n and chitosan concentration further improved their paste-like quality (Figure 2d, e and Table 3), which is desired for implantation during surgery. Chitosan-PRP formulations coagulated more rapidly than recalcified PRP (Figure 3), and increasing chitosan M_n and chitosan concentration decreased the clot reaction time (R) of the mixtures (Figure 3a, b and Table 3). Formulations containing low

chitosan M_n and concentration had lower clot maximal amplitude than PRP-only clots (Figure 3d, e), and increasing lyoprotectant concentration in the freeze-dried cakes decreased clot strength (Figure 3f and Table 3). The solid chitosan-PRP hybrid clots retracted much less than PRP controls (Figure 3), almost entirely blocking the 5 x retraction seen in PRP alone. The formulations containing the highest chitosan and lyoprotectant concentrations were the most stable and least retracting (Figure 3 and Table 3).

3.4. Chitosan M_n affects hybrid clot homogeneity

Chitosan distribution in the hybrid clots was strongly dependent on the chitosan M_n , with medium M_n chitosan yielding homogenous clots (Figure 4c, d). Large chitosan

Table 2B. pH of formulations post reconstitution with PPP. Data are presented as mean \pm SD. n was between 3 and 13 for each formulation. As expected, pH in chitosan-PPP mixtures was lower than PPP or PRP alone

| Lyopro-tectant concentration | Chitosan concentration 0.56% w/v | | Chitosan concentration 1% w/v | | Freshly isolated PPP | Freshly isolated PRP |
|------------------------------|----------------------------------|-----------------|-------------------------------|-----------------|----------------------|----------------------|
| | Trehalose | Mannitol | Trehalose | Mannitol | | |
| 1% w/v | 7.11 \pm 0.07 | N/D | 6.80 \pm 0.02 | N/D | | |
| 2% w/v | 6.94 \pm 0.06 | 6.97 \pm 0.08 | 6.78 \pm 0.10 | 6.79 \pm 0.11 | 7.81 \pm 0.23 | 7.90 \pm 0.23 |
| 4% w/v | 6.96 \pm 0.11 | 6.84 \pm 0.06 | 6.90 \pm 0.12 | 6.97 \pm 0.03 | | |
| 6% w/v | 6.88 \pm 0.15 | 6.94 \pm 0.10 | 6.75 \pm 0.15 | 6.93 \pm 0.35 | | |

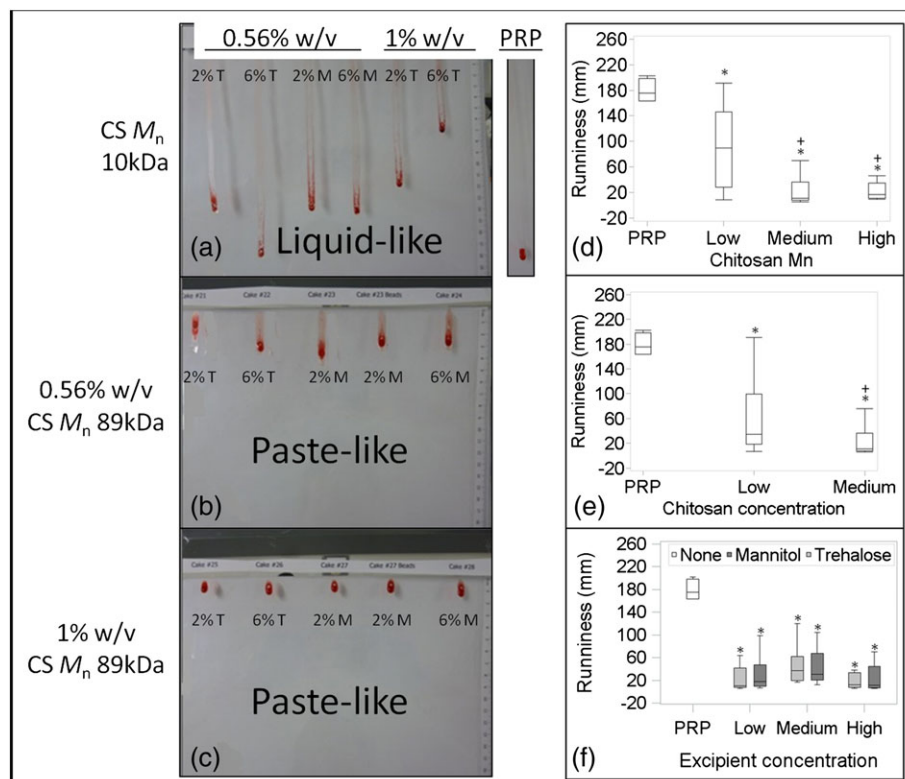


Figure 2. Examples of the runniness test on an inclined plastic plate, to assess the paste-like properties of the different chitosan-PRP formulations (panels a–c). Chitosan-PRP formulations were more paste-like than those with PRP alone (panels a and d–f). Increasing chitosan M_n and chitosan concentration improved the paste-like properties of chitosan-PRP formulations (panels d and e), while increasing lyoprotectant concentration did not have an effect (panel f). T, trehalose; M, mannitol. n was 3–13 for each formulation. * $p < 0.05$ compared to PRP. + $p < 0.05$ compared to the 'Low' category. Chitosan M_n was low (4–11 kDa), medium (28–56 kDa) or high (79–54 kDa) for freeze-dried formulations (panel d). Chitosan concentration was low (0.56% w/v) or medium (1% w/v) for freeze-dried formulations (panel e). Lyoprotectant concentration was low (1% or 2% w/v), medium (4% w/v) or high (6% w/v) for freeze-dried formulations (panel f). Note that water has runniness exceeding 310 mm. [Colour figure can be viewed at wileyonlinelibrary.com]

Table 3. Pearson correlation coefficients r and corresponding p values between the different performance criteria assessed *in vitro* or *in vivo* and chitosan M_n , chitosan concentration and lyoprotectant concentration. Strong and moderate significant correlations are in bold. Increasing chitosan M_n and concentration improved paste-like properties of freeze-dried formulations and decreased the clot reaction time. Formulations containing high concentrations of lyoprotectants had lower clot strength and corresponding clot maximal amplitude. Increasing chitosan and lyoprotectant concentration increased clot stability and led to less mass lost from hybrid clots

| | Chitosan M_n | Chitosan concentration | Lyoprotectant concentration |
|--|----------------------|------------------------|-----------------------------|
| Runniness | -0.53075 < 0.0001 | -0.56671 < 0.0001 | -0.26086 0.0120 |
| Clot reaction time | -0.44367 < 0.0001 | -0.41888 < 0.0001 | -0.14580 0.1217 |
| Clot maximal amplitude | -0.07092 0.4534 | -0.07024 0.4577 | -0.63634 < 0.0001 |
| Clot mass lost | -0.19287 0.0398 | -0.76032 < 0.0001 | -0.59950 < 0.0001 |
| Vv nucleated cells <i>in vivo</i> | -0.02277 0.8891 | -0.00611 0.9709 | -0.08639 0.5961 |
| Vv RAM11-positive macrophages <i>in vivo</i> | -0.03435 0.7761 | 0.04219 0.7015 | 0.13232 0.2218 |

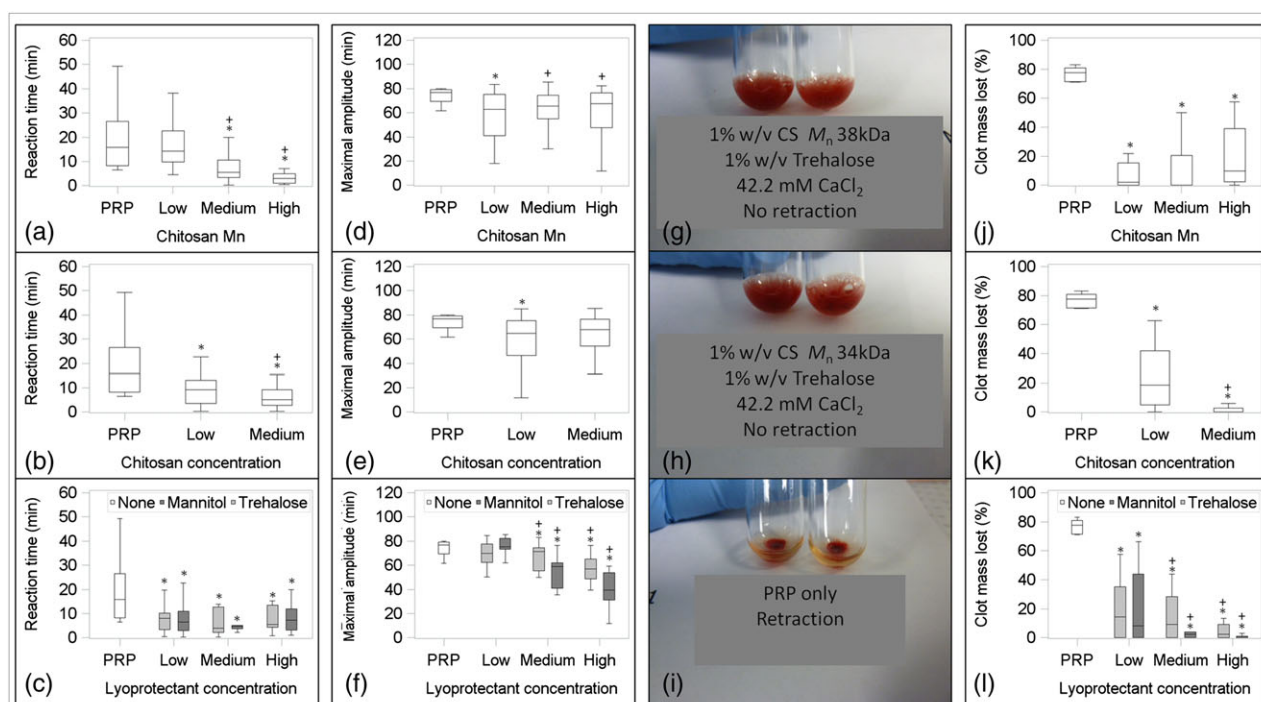


Figure 3. Increasing chitosan M_n and chitosan concentration decreased clot reaction time of chitosan-PRP formulations (panels a and b), while increasing lyoprotectant concentration had no effect (panel c). Hybrid clot maximal amplitude corresponding to clot strength was similar to that for PRP alone for formulations containing chitosan of higher M_n and higher concentration (panels d and e). Increasing lyoprotectant concentration decreased clot maximal amplitude (panel f). Chitosan-PRP hybrids remained voluminous after clotting for 1 h at 37°C (panels g and h), while PRP-only clots retracted significantly and exuded serum (panel i). Increasing chitosan and lyoprotectant concentration decreased liquid expression (panels j-l). * $p < 0.05$ compared to PRP. + $p < 0.05$ compared to the 'Low' category. Chitosan M_n was low (4–11 kDa), medium (28–56 kDa) or high (79–154 kDa) for freeze-dried formulations (panels a, d and j). Chitosan concentration was low (0.56% w/v) or medium (1% w/v) for freeze-dried formulations (panels b, e and k). Lyoprotectant concentration was low (1% or 2% w/v), medium (4% w/v) or high (6% w/v) for freeze-dried formulations (panels c, f and l). [Colour figure can be viewed at wileyonlinelibrary.com]

aggregates were seen in hybrid clots containing chitosans of high M_n (Figure 4a, b), while using chitosan of low M_n in the freeze-dried cakes resulted in phase separation of the polymer and PRP (Figure 4e, f).

3.5. Chitosan-PRP implants reside for at least 14 days *in vivo*, induce cell recruitment and have tissue building capacity

Chitosan-PRP hybrid clots were resident until at least 2 weeks *in vivo* (Figure 5a–d), while PRP controls were quickly degraded and mainly gone within 1 day

(Figure 5e–g). Chitosan-PRP implants, but not the PRP-only controls, induced cell recruitment (compare Figure 5a–d compared to e–g). These included round and elongated mononuclear cells as well as polymorphonuclear cells (Figure 5k, l). Cells accumulated first at the periphery of the implants and then gradually invaded the center of the implants (Figure 5a–d and k, l). There was no effect of chitosan M_n , chitosan concentration or lyoprotectant concentration on early cell recruitment to the implants (Figure 5m–o). Chitosan was internalized and degraded by host cells, as revealed by epifluorescence microscopy (Figure 5p, q). There was no histological evidence of cell necrosis at 1 to 3 days post

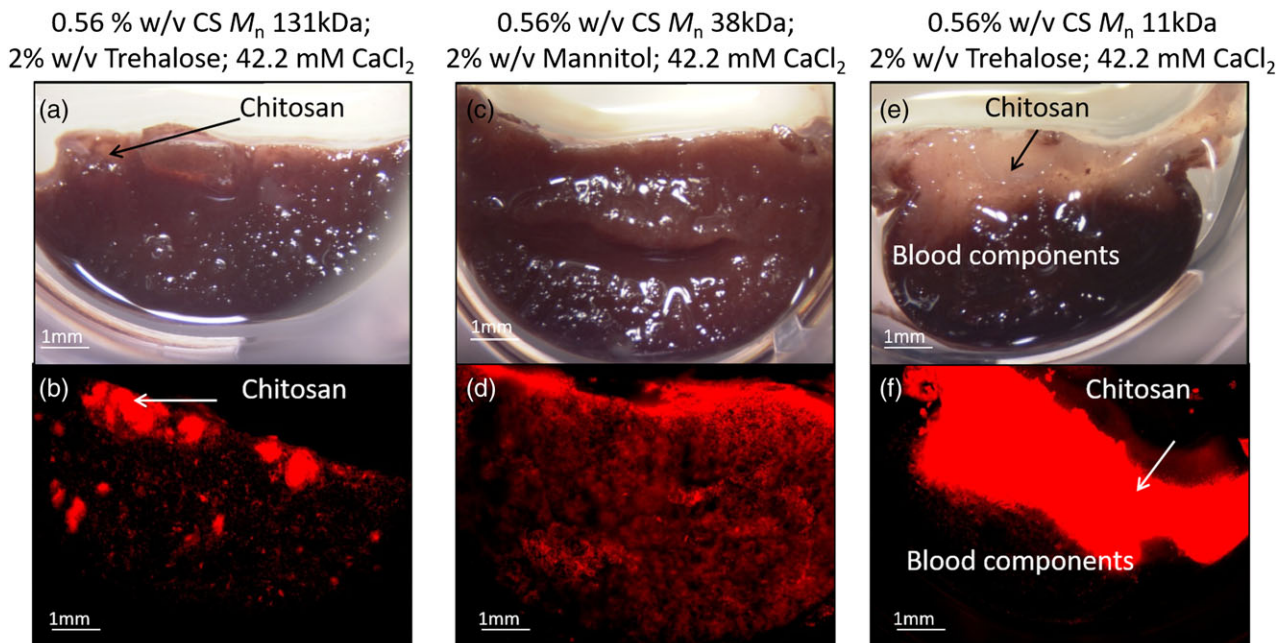


Figure 4. Chitosan dispersion in the hybrid clots was homogenous when chitosan of medium M_n was used to prepare freeze-dried formulations (panels c and d). Large chitosan aggregates were apparent in formulations containing chitosan of high M_n (panels a, b), while phase separation was seen for formulations prepared with chitosan of low M_n (panels e, f). Chitosan can be detected with red fluorescent microscopy since a rhodamine-chitosan tracer of similar M_n was added to each freeze-dried formulation for imaging purposes. [Colour figure can be viewed at wileyonlinelibrary.com]

implantation in any of the formulations tested, while sparse fragmented nuclei were observed at 7 and 14 days. Chitosan-GP/blood implants had a biodegradation rate, cell recruitment potential and effect on viability similar to that of chitosan-PRP implants (Figure 5h–j and m–o).

Chitosan-PRP implants induced recruitment of RAM11-positive macrophages starting from day 7 post implantation, where they accumulated at the periphery of the implants (Figure 6a, b and e, f). Only a small number of macrophages had invaded the centre of the implants by day 14 post implantation (Figure 6e, f), so panels i to k are showing Vv of RAM11-positive cells at the edges of the implants only. No RAM11-positive macrophages were observed in the PRP-only controls (Figure 6c, d). Chitosan-PRP implants also induced angiogenesis in subcutaneous tissues (Figure 6g, h). There was no significant effect of chitosan M_n , chitosan concentration or lyoprotectant concentration on macrophage recruitment to the implants (Figure 6i–k and Table 3). Chitosan-GP/blood implants recruited a similar number of macrophages as freeze-dried chitosan-PRP implants (Figure 6i–k) and also induced angiogenesis.

4. Discussion

The purpose of this study was to identify freeze-dried chitosan formulations that can be solubilized in PRP to yield injectable coagulating implants for tissue repair in orthopaedics. Ideally, freeze-dried cakes would be rapidly and completely solubilized in PRP (< 1 min), would have paste-like handling properties upon solubilization and would coagulate rapidly (< 5 min) to form solid

homogenous space-filling chitosan-PRP hybrid implants that exhibit residency and bioactivity *in vivo*. Critical properties of the freeze-dried cakes, such as chitosan M_n , chitosan concentration and lyoprotectant concentration, were found to control the performance characteristics of the solubilized chitosan-PRP mixtures, thus confirming our first hypothesis. These properties could be tailored to each tissue repair application to meet the requirements of a specific procedure. As was hypothesized, there was an upper limit of chitosan M_n and chitosan concentration above which the freeze-dried cakes became non-soluble (Figure 1). One of our aims here was to preserve the ability of PRP to be activated by the calcium chloride present in the freeze-dried cake to initiate coagulation, as is presently done in some clinical applications of PRP (Zumstein *et al.*, 2011). The presence of lyoprotectants in the cakes was a concern in that respect, since sugars and polyols have been found previously to impair normal hemostatic mechanisms (Bakaltcheva and Reid, 2003; Bakaltcheva *et al.* 2007; Lindroos *et al.*, 2010; Luostarinen *et al.*, 2011). We found that coagulation was in fact impaired when lyoprotectant concentration exceeded a certain threshold (Figure 1). We therefore elected to restrict the lyoprotectant concentration in the cakes to 6% *w/v* and below.

The poor stability of solution-based chitosan systems is well known and has been an ongoing challenge in the pharmaceutical and biomedical fields (Szymanska and Winnicka, 2015). Chitosan inevitably undergoes hydrolysis in the presence of acids (Varum *et al.*, 2001) and several sterilization methods, such as steam sterilization and irradiation, have been shown to also degrade the polymer (Jarry *et al.*, 2001; Yang *et al.*, 2007). The use of freeze-drying will effectively increase

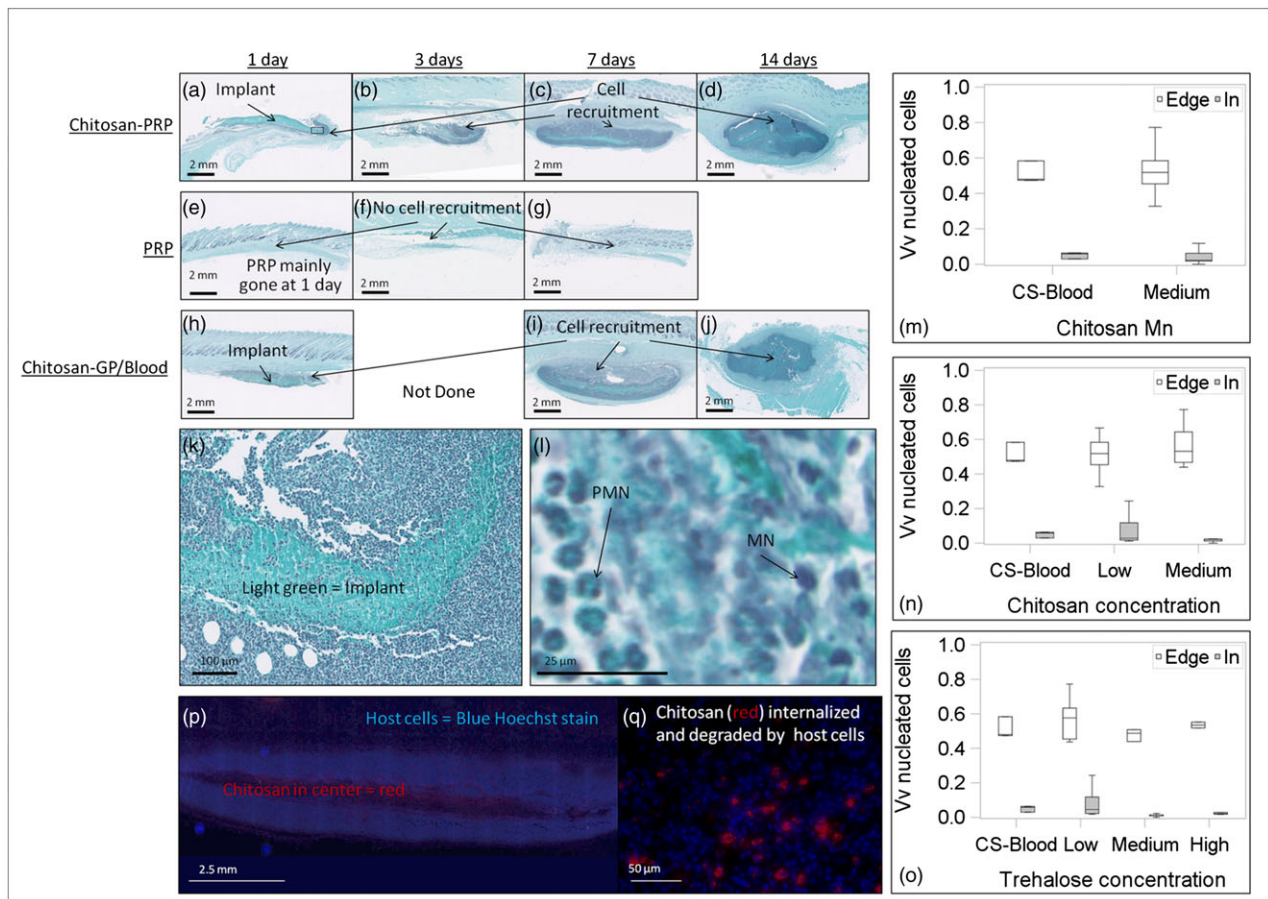


Figure 5. Chitosan-PRP implants were injected subcutaneously into NZW rabbits and were resident *in vivo* for at least 14 days (panels a–d), while PRP controls were quickly degraded (panels e–g). Chitosan-PRP implants, but not the PRP controls, induced cell recruitment (compare panels a–d to panels e–g). These included round, elongated mononuclear cells (MN) as well as polymorphonuclear cells (PMN) (panels k, l). Cells initially accumulated at the edges of the chitosan-PRP implants and gradually migrated towards the centre of the implants (panels a–d and k). Vv of nucleated cells was, therefore, greater at the edge of implants compared to inside implants at day 1 (panels m–o). Formulations in panels a–d and k–l contain 1% (w/v) chitosan of medium M_n (28–56 kDa), 2% (w/v) trehalose and 42.2 mM CaCl_2 . Rectangle in panel a shows where higher magnification images k and l were acquired. There was no effect of chitosan M_n , chitosan concentration or lyoprotectant concentration on early cell recruitment to the implants (panels m–o). Chitosan M_n was medium (28–56 kDa) for freeze-dried formulations and ~150 kDa for CS-Blood (m). Chitosan concentration was low (0.56% w/v) or medium (1% w/v) for freeze-dried formulations and 0.42% w/v for CS-Blood (n). Trehalose concentration was low (1% or 2% w/v), medium (4% w/v) or high (6% w/v) for freeze-dried formulations while CS-Blood was devoid of trehalose (panel o). Chitosan-PRP implants were degraded by host cells without any adverse reactions (panels p and q). Chitosan can be detected with red fluorescent microscopy in panels p and q since a rhodamine-chitosan tracer of similar M_n was added to each freeze-dried formulation for imaging purposes. Chitosan-GP/Blood implants (containing 0.42% w/v chitosan, ~150 kDa and no lyoprotectant) had a biodegradation rate and cell recruitment potential similar to that of chitosan-PRP implants (panels h–j and m–o). [Colour figure can be viewed at wileyonlinelibrary.com]

the stability and shelf-life of chitosan-based products, and stability studies in a controlled environment are ongoing. Our low M_n and medium M_n chitosan solutions were easily sterilized by filtration, resolving one important practical issue. Terminal sterilization of the freeze-dried cakes may be another option when large-scale production becomes required. Other authors have described lyophilized scaffolds composed of chitosan and PRP (Kutlu *et al.*, 2013; Shimojo *et al.*, 2015; Shimojo *et al.*, 2016). These formulations were solid and it is our understanding that they were designed to remain so for implantation. To our knowledge, there are no publications to date describing the direct solubilization of freeze-dried chitosan formulations in PRP to form injectable implants that coagulate *in situ*.

Increasing chitosan M_n and chitosan concentration in the freeze-dried cakes improved the paste-like properties of the chitosan-PRP mixtures, thus confirming our second hypothesis (Figure 2). Increasing chitosan M_n and chitosan concentration also decreased the clot reaction time of the chitosan-PRP mixtures, to a value significantly

lower than that of PRP (Figure 3), which is a significant clinical advantage when applying these implants during surgical procedures when time is of the essence. This is in contrast to chitosan-GP/blood implants which have been shown to have a clot reaction time similar to that of whole blood (Marchand *et al.*, 2009). High lyoprotectant concentrations decreased clot maximal amplitudes (Figure 3) reflecting a weakened clot structure; however, additional studies are required to elucidate the solidification mechanisms of chitosan-PRP and the way chitosan M_n , chitosan concentration and lyoprotectant concentration modulate those mechanisms. PRP-only clots expressed large quantities of serum post coagulation and lost up to 80% of their original mass (Figure 3). This strong clot retraction is mediated by platelets and is also influenced by the hematocrit level (Chao *et al.*, 1976; Cohen *et al.*, 1982; Brass *et al.*, 2005). It is thus not surprising that PRP clots, which contain only a fraction of erythrocytes, would express more serum than whole blood clots, previously reported at ~40% for human blood (Hoemann *et al.*, 2007).

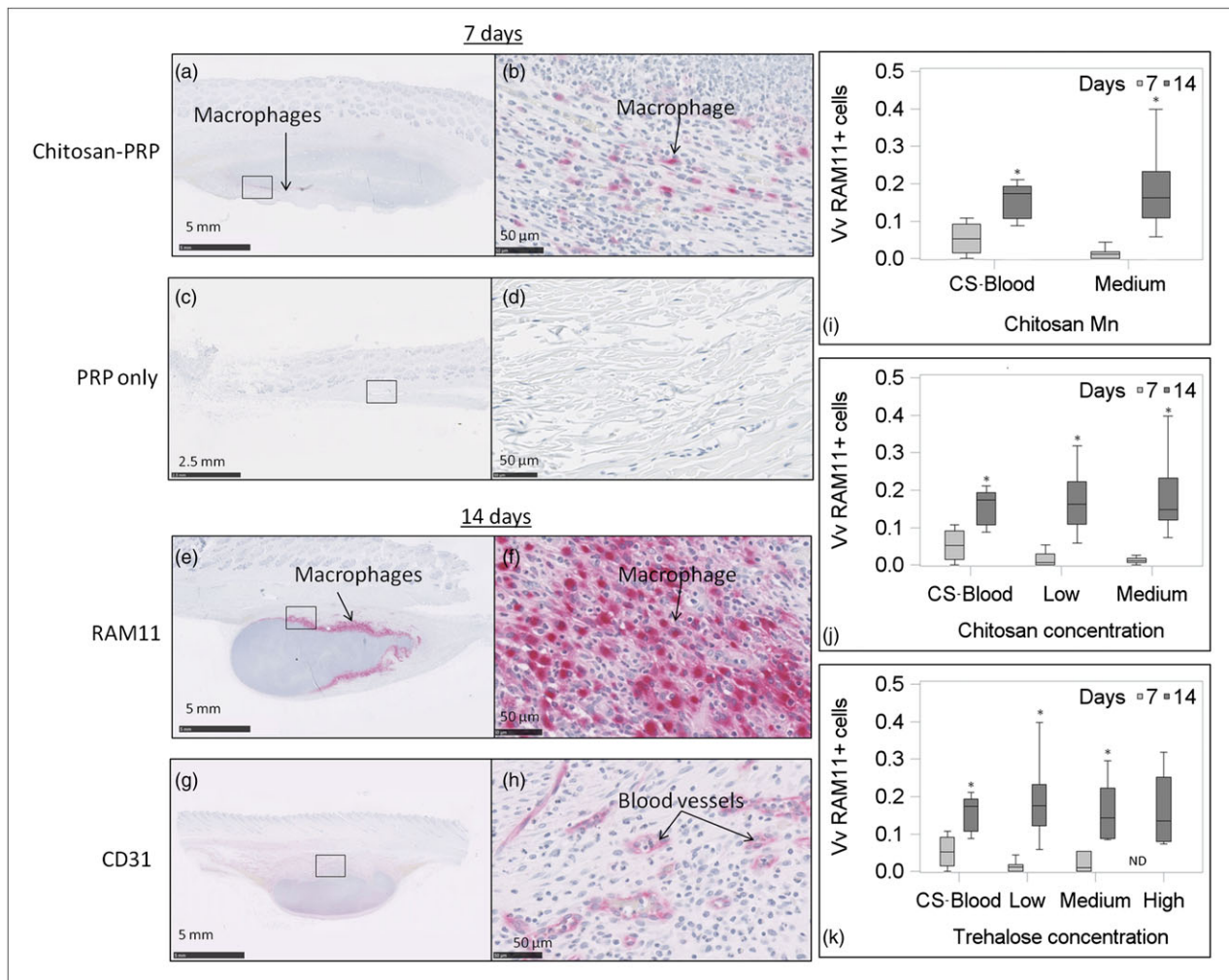


Figure 6. Chitosan-PRP implants induced RAM11-positive macrophage recruitment at days 7 (panels a, b) and 14 (panels e, f), where they accumulated at the edges of the implants. A subset of these macrophages is expected to be alternatively-activated macrophages. No RAM11-positive macrophages were recruited to the PRP-only controls (panels c, d). Chitosan-PRP implants also induced angiogenesis in subcutaneous tissues (panels g, h). Panels a, b and e, f show chitosan-PRP formulations composed of 1% (w/v) chitosan M_n 50 kDa with 1% trehalose and 42.2 mM CaCl_2 . Rectangles in panels a, c, e and g indicate regions in which the higher magnification images b, d, e and h were taken. The volume density (Vv) of RAM11-positive macrophages recruited to the periphery of freeze-dried chitosan-PRP implants increased with time (from days 7 to 14 in panels i–k). There was no effect of chitosan M_n , chitosan concentration or lyoprotectant concentration on macrophage recruitment to the implants (panels i–k). Chitosan-GP/Blood implants (CS-Blood) had an effect on macrophage recruitment similar to that of chitosan-PRP implants (panels i–k). * $p < 0.05$ compared to day 7. ND = Not done. Chitosan M_n was medium (28–56 kDa) for freeze-dried formulations and ~ 150 kDa for CS-Blood (panel i). Chitosan concentration was low (0.56% w/v) or medium (1% w/v) for freeze-dried formulations and 0.42% w/v for CS-Blood (panel j). Trehalose concentration was low (1% or 2% w/v), medium (4% w/v) or high (6% w/v) for freeze-dried formulations, while CS-Blood was devoid of trehalose (panel k). [Colour figure can be viewed at wileyonlinelibrary.com]

Chitosan-PRP hybrid clots, on the other hand, remained physically stable upon coagulation (Figure 3), similar to chitosan-GP/blood clots (Hoemann *et al.*, 2007). Preliminary confocal and electron microscopy studies suggest that chitosan is able to coat the platelets, the fibrin network and to partly inhibit platelet aggregation (unpublished observations) in chitosan hybrid clots. Therefore, increasing chitosan concentration in the hybrid clots would be expected to further inhibit clot retraction, as was seen here in this study (Figure 3).

Chitosan dispersion in the hybrid clots was strongly dependant on chitosan M_n and was homogenous only when medium M_n chitosans were used (Figure 4), leading us to choose medium M_n chitosans for *in vivo* testing (Table 1). As expected, freeze-dried cakes containing high lyoprotectant concentrations had high osmolality upon reconstitution (Table 2A) but, contrary to our third hypothesis, this did not induce cell necrosis/death upon

in vivo implantation, as assessed histologically. The performance of the different freeze-dried formulations was similar in this subcutaneous model. *In vivo* responses to chitosan-PRP implants were significant since these implants resided until at least 14 days post implantation and induced cell recruitment and angiogenesis during this period (Figures 5 and 6). In contrast, PRP-only controls degraded rapidly and had little bioactivity (Figures 5 and 6). It is currently unclear what proportion of this increased biological activity displayed by chitosan-PRP implants is due to their physical stability and the subsequent sustained release of platelet-derived growth factors or due to intrinsic properties of the chitosan itself. Studies of the release profiles of chitosan-PRP clots are underway and will clarify the release kinetics of platelet factors from chitosan-PRP clots. The *in vivo* residency and cell recruitment potential of the chitosan-PRP implants in subcutaneous sites were similar to those of

chitosan-GP/blood implants, as seen in the current study (Figures 5 and 6) and in a previously published study (Hoemann *et al.*, 2010). It thus appears reasonable to assume that the positive effects exerted by chitosan-GP/blood implants on cartilage repair (Hoemann *et al.*, 2005; Hoemann *et al.*, 2007; Stanish *et al.*, 2013; Shive *et al.*, 2015) would be seen also with these freeze-dried chitosan-PRP implants.

Although we postulate that the runniness data could be interpreted as a viscosity measurement, one limitation of this study is that no mechanical or viscosity measurement was performed on the chitosan-PRP formulations and coagulated hybrids. Another limitation is the low number of animals used for the *in vivo* study and the short time points assessed. In addition, multiple injections of different formulations were performed on each animal in order to reduce animal numbers. We are currently testing these chitosan-PRP implants in pre-clinical cartilage, meniscus and rotator cuff repair models and expect that repair outcomes will be improved as compared to current clinical treatments.

In summary, freeze-dried chitosan formulations can be solubilized in PRP to form injectable coagulating biodegradable and biocompatible implants for tissue repair applications. The properties of the hybrid implants can be modulated by selecting the chitosan molar mass (M_n), chitosan concentration and lyoprotectant concentration in the freeze-dried cakes. Unlike PRP alone, these hybrid implants are physically stable and persist *in vivo* so that they are expected to significantly prolong bioactivity for tissue repair. Future indications for

chitosan-PRP implants include meniscus repair, cartilage repair and rotator cuff repair.

Conflict of interest

A. C., V. D., D. V., M. L., C. D. H. and M. D. B. hold shares and C. D. H. and M. D. B. are Directors of Ortho Regenerative Technologies Inc.

Acknowledgments

We acknowledge the technical contributions of Érika Miller-Jolicoeur, Constanze Neumann and Pauline Porquet. We also acknowledge the funding sources, Canadian Institutes of Health Research (Grant #MOP 115186), Canada Foundation for Innovation, Groupe de Recherche en Sciences et Technologies Biomédicales, Natural Sciences and Engineering Research Council of Canada, and the assistance of Ortho Regenerative Technologies Inc.

Author contributions

The following authors contributed to the conception and design of the study (A. C., V. D., M. L., C. D. H., M. D. B.), to acquisition of data (A. C., V. D., G. P., M. N., D. V., M. L.), to analysis and interpretation of the data (A. C., V. D., D. V., M. L., C. D. H., M. D. B.), to drafting and revising the article (A. C., V. D., D. V., M. L., C. D. H., M. D. B.) and M. D. B. gave final approval of the manuscript

References

- Ahmad Z, Howard D, Brooks RA, *et al.* 2012; The role of platelet rich plasma in musculoskeletal science. *JRSM Short Rep* **3**: 40.
- Anitua E, Aguirre JJ, Algorta J, *et al.* 2008; Effectiveness of autologous preparation rich in growth factors for the treatment of chronic cutaneous ulcers. *J Biomed Mater Res B Appl Biomater* **84**: 415–421.
- Bakaltcheva I, O'Sullivan AM, Hmel P, Ogbu H. 2007; Freeze-dried whole plasma: Evaluating sucrose, trehalose, sorbitol, mannitol and glycine as stabilizers. *Thromb Res* **120**: 105–116.
- Bakaltcheva I, Reid T. 2003; Effects of blood product storage protectants on blood coagulation. *Transfus Med Rev* **17**: 263–271.
- Brass LF, Zhu L, Stalker TJ. 2005; Minding the gaps to promote thrombus growth and stability. *J Clin Invest* **115**: 3385–3392.
- Chahal J, Van Thiel GS, Mall N, *et al.* 2012; The Role of Platelet-Rich Plasma in Arthroscopic Rotator Cuff Repair: A Systematic Review With Quantitative Synthesis. *Arthroscopy* **28**: 1718–1727.
- Chao FC, Shepro D, Tullis JL, Belamirich FA, Curby WA. 1976; Similarities between platelet contraction and cellular motility during mitosis: role of platelet microtubules in clot retraction. *J Cell Sci* **20**: 569–588.
- Chen G, Sun J, Lascau-Coman V, Chevrier A, Marchand C, Hoemann CD. 2011; Acute Osteoclast Activity following Subchondral Drilling Is Promoted by Chitosan and Associated with Improved Cartilage Repair Tissue Integration. *Cartilage* **2**: 173–185.
- Chenite A, Chaput C, Wang D, *et al.* 2000; Novel injectable neutral solutions of chitosan form biodegradable gels in situ. *Biomaterials* **21**: 2155–2161.
- Chevrier A, Hoemann CD, Sun J, Buschmann MD. 2007; Chitosan-glycerol phosphate/blood implants increase cell recruitment, transient vascularization and subchondral bone remodeling in drilled cartilage defects. *Osteoarthritis Cartil* **15**: 316–327.
- Cohen I, Gerrard JM, White JG. 1982; Ultrastructure of clots during isometric contraction. *J Cell Biol* **93**: 775–787.
- Griffin JW, Hadeed MM, Werner BC, Diduch DR, Carson EW, Miller MD. 2015; Platelet-rich Plasma in Meniscal Repair: Does Augmentation Improve Surgical Outcomes? *Clin Orthop Relat Res* **473**: 1665–1672.
- Griffiths G. 1993; Quantitative aspects of immunocytochemistry. Fine Structure Immunocytochemistry Springer-Verlag, Berlin, 371–445.
- Hoemann CD, Chen G, Marchand C, *et al.* 2010; Scaffold-Guided Subchondral Bone Repair Implication of Neutrophils and Alternatively Activated Arginase-1+ Macrophages. *Am J Sports Med* **38**: 1845–1856.
- Hoemann CD, Hurtig M, Rossomacha E, *et al.* 2005; Chitosan-glycerol phosphate/blood implants improve hyaline cartilage repair in ovine microfracture defects. *J Bone Joint Surg Am* **87A**: 2671–2686.
- Hoemann CD, Sun J, McKee MD, *et al.* 2007; Chitosan-glycerol phosphate/blood implants elicit hyaline cartilage repair integrated with porous subchondral bone in microdrilled rabbit defects. *Osteoarthritis Cartil* **15**: 78–89.
- Jarry C, Chaput C, Chenite A, Renaud MA, Buschmann M, Leroux JC. 2001; Effects of steam sterilization on thermogelling chitosan-based gels. *J Biomed Mater Res* **58**: 127–135.
- Kon E, Filardo G, Di Matteo B, Marcacci M. 2013; PRP for the treatment of cartilage pathology. *Open Orthop J* **7**: 120–128.
- Kutlu B, Tigli Aydin RS, Akman AC, Gumusderelioglu M, Nohutcu RM. 2013; Platelet-rich plasma-loaded chitosan scaffolds: preparation and growth factor release kinetics. *J Biomed Mater Res B* **101**: 28–35.
- Lavertu M, Filion D, Buschmann MD. 2008; Heat-induced transfer of protons from chitosan to glycerol phosphate produces chitosan precipitation and gelation. *Biomacromolecules* **9**: 640–650.
- Lavertu M, Xia Z, Serreqi AN, *et al.* 2003; A validated ¹H NMR method for the determination of the degree of deacetylation of chitosan. *J Pharm Biomed Anal* **36**: 1149–1158.
- Lindroos A-C, Schramko A, Tanskanen P, Niemi T. 2010; Effect of the Combination of Mannitol and Ringer Acetate or Hydroxyethyl Starch on Whole Blood Coagulation In Vitro. *Neurosurg Anesthesiol* **22**: 16–20.
- Lu HH, Vo JM, Chin HS, *et al.* 2008; Controlled delivery of platelet-rich plasma-derived growth factors for bone formation. *J Biomed Mater Res A* **86**: 1128–1136.
- Luostarinen T, Niya T, Schramko A, Rosenberg P, Niemi T. 2011; Comparison of Hypertonic Saline and Mannitol on Whole Blood Coagulation In Vitro Assessed by Thromboelastometry. *Neurocrit Care*, **14**: 238–243.
- Ma O, Lavertu M, Sun J, *et al.* 2008; Precise derivatization of structurally distinct chitosans with rhodamine B isothiocyanate. *Carbohydr Polym* **72**: 616–624.
- Marchand C, Rivard GE, Sun J, Hoemann CD. 2009; Solidification mechanisms of chitosan-glycerol phosphate/blood implant for articular cartilage repair. *Osteoarthritis Cartil* **17**: 953–960.
- Nguyen S, Winnik FM, Buschmann MD. 2009; Improved reproducibility in the determination of the molecular weight of chitosan by analytical size exclusion chromatography. *Carbohydr Polym* **75**: 528–533.
- Nguyen TTB, Hein S, Ng CH, Stevens WF. 2008; Molecular stability of chitosan in acid solutions stored at various conditions. *J Appl Polym Sci* **107**: 2588–2593.
- Shimojo AA, Perez AG, Galdames SE, Brissac IC, Santana MH. 2015; Performance of PRP associated with

- porous chitosan as a composite scaffold for regenerative medicine. *ScientificWorld Journal* **2015**: 396131.
- Shimojo AA, Perez AG, Galdames SE, Brissac IC, Santana MH. 2016; Stabilization of porous chitosan improves the performance of its association with platelet-rich plasma as a composite scaffold. *Mater Sci Eng C Mater Biol Appl* **60**: 538–546.
- Shive MS, Stanish WD, McCormack RG, *et al.* 2015; BST-CarGel® Treatment Maintains Cartilage Repair Superiority over Microfracture at 5 Years in a Multicenter Randomized Controlled Trial. *Cartilage* **6**, 4: 62–72.
- Stanish WD, McCormack RG, Forriol F, *et al.* 2013; Novel Scaffold-Based BST-CarGel Treatment Results in Superior Cartilage Repair Compared with Microfracture in a Randomized Controlled Trial. *J Bone Joint Surg Am* **95A**: 1640–1650.
- Szymanska E, Winnicka K. 2015; Stability of Chitosan-A Challenge for Pharmaceutical and Biomedical Applications. *Mar Drugs* **13**: 1819–1846.
- Varum KM, Ottoy MH, Smidsrod O. 2001; Acid hydrolysis of chitosans. *Carbohydr Polym* **46**: 89–98.
- Yang Y-M, Zhao Y-H, Liu X-H, Ding F, Gu X-S. 2007; The effect of different sterilization procedures on chitosan dried powder. *J Appl Polym Sci* **104**: 1968–1972.
- Zumstein MA, Bielecki T, Ehrenfest DMD. 2011; The Future of Platelet Concentrates in Sports Medicine: Platelet-Rich Plasma, Platelet-Rich Fibrin, and the Impact of Scaffolds and Cells on the Long-term Delivery of Growth Factors. *Oper Tech Sports Med* **19**: 190–197.